Bulletin of Earth Sciences of Thailand

Contrasting Depositional and Diagenetic Complexity in Deep and Shallow Water Successions in the Permian Carbonates of Pak Chong Region, Central Thailand

Maryam Mirzaloo

Petroleum Geoscience Program, Department of Geology, Faculty of Science,
Chulalongkorn University, Bangkok 10330, Thailand
Corresponding author email: maryam.mirzaloo@yahoo.com

Abstract

Permian platform and basin complexes are well developed in the Saraburi area, central Thailand, but no detailed direct isotope and petrographic comparison of depositional and diagenetic evolution has been made between sediments deposited in these various shallow and deep water associations. Three geographically separate regions were chosen for detailed field and laboratory study.

Site 1 (shallow water carbonate platform mound) sediment was constructed by a combination of cementstone and microbial boundstones, with associated coral, algal, crinoid and sponge assemblages.

Site 2 (outer platform/Upper slope) sediments are dominated by beds and breccias composed of varying combinations of bioclast-rich pack/grainstone and microbial pack/grainstones. The site 2 facies show textures that are variably pressurized and fluidized, but still entrain clasts derived from sediment sources similar to those being deposited at site 1. Site 3 deposits are interpreted as debris flow and mud flow deposits, associated with upper slope instability and are a combination marine mixed siliciclastic–carbonate beds, deposited at the toe of slope and interlayered with hemipelagic muds and basinal shales.

Main types of calcite cements are bladed, sparry calcite mosaic, fibrous, syntaxial overgrowth and blocky (some with a ferroan-calcite component). Stable isotope analyses show a covariant burial-related trend between $\delta^{18}O$ and $\delta^{13}C$ from (−4.14 to −24.7) and (+ 0.2 to +5.3) ‰ VPDB respectively, there is a secondary trend towards depleted carbon values between −0.2 and −7 ‰ VPDB respectively. Negative oxygen values are related to higher temperatures and hydrothermal fluid. The carbon-depletion trend may be associated with either catagenic evolution of organic matter in the burial environment, or earlier overprint of marine microbial productivity .

Diagenetic signatures in these carbonates suggest that marine diagenetic fluids dominated in formation of the various earlier calcite cements, but that deep burial diagenesis also played its role. The transition in cement isotope signatures is controlled by the fact that the depositional environment evolved, with burial, into a complex tectonic subsurface regime, where across all three sites a common set of burial-related calcites formed.

Keywords: Carbonate, Permian,shallow water paltform, slope, deepwater basin, diagenetic fluid

1. Introduction

Studies of the sedimentology of the Saraburi Group are few. This study aims to document and compare depositional and diagenetic evolution across what are likely; a) Platform mound, b) Outer platform-Upper slope, and 3) Basinal locations in central Thailand in what is now a region adjacent to the main Indosinian suture belt (Figure 1). This investigation focuses on the evolution of primary and secondary sedimentary features through time, burial and uplift, by documenting similarities and differences in early to late diagenesis within shallow to deep water successions of Permian carbonate sequences in central Thailand.

2. Location

Three investigated outcrops were chosen, situated near the cities of Muak Lek and Pak Chong cities (Fig.1). Site 1 is situated on a road cut and consist of fractured 85 m section of thick bedded grey limestone cross-cut by various sets of joints, fractures and clastic dykes and pipes, and volcanic rock debris. Site 2 is located near to the Site 1 and is made up of numerous soft-sediment deformation structures and breccias, which are hosted within a 69 m thick package of bedded grey limestones with chert nodules. Site 3 is centered in an aggregate quarry, about 30 km from the site 1 &2. The quarry walls expose a section of marine mixed siliciclastic–carbonate deep water sediments.

3. Methods

The sampling and interpretation framework for this study is based onthree measured and mapped geological sections. the occurrence, style and orientation of bedding, fractures, and veins was mapped and measuring across these natural exposure. A total of 98 representative samples were gathered from the 3 sites, slab-cut and photographed. 10 samples were submitted for semi-quantitative XRD determination and 15 representative samples were chosen for standard thin-section petrographic analysis. Fossil fragments, lime mud matrices, carbonate matrix, breccia fragments, calcite grains/fragments

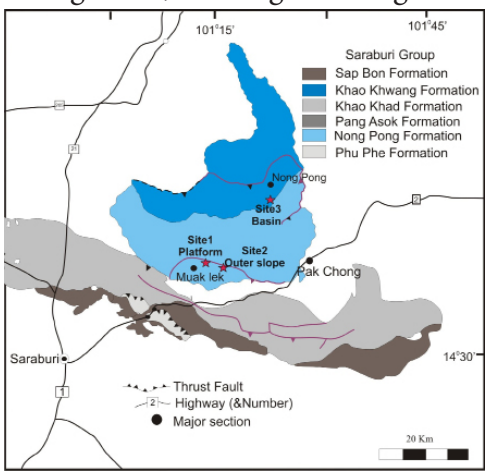

Figure 1. Study area location

and spars, calcite-filled veins/fractures, and possible neptunian dykes and injection features were drilled out using the narrowest bit sizes available for a superior standard dental technician's drill. Powders from 128 samples were collected and submitted to the isotope

lab at Monash University Australia. Basic composition and classification were done according to the Embry and Klovan's (1972) modifi cation of Dunham's original carbonate rock classification.

4. Key depositional features

Site 1/Platform *mound setting:*

Boundstones with a packstone matrix, dominated by small shell fragments of corals, crinoid debris and calcareous algal fragments, combine

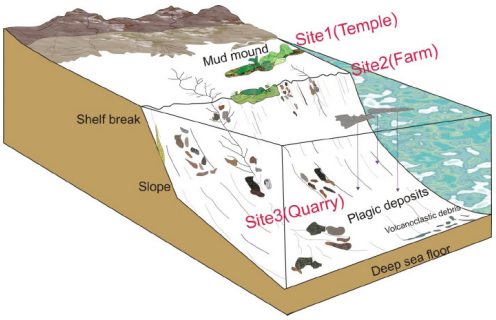

Figure 2. Depositional reconstruction of three sites.

to form a facies mosaic in the outcrop, which passes laterally in places into coarser-grained grainstones, also dominated by shell fragments composed of crinoid debris, foraminifera, bryozoans, corals, calcareous algae and gastropods (Fig.3). In several places there are irregularly-shaped cement-lined dykes, pipes and fracture fills (1 to 6cm across) that, along with their cement linings, are locally filled with brown-coloured sediment. Site 1 strikes 219° and dips 60°.

Site2/outer platform-upper slope:

Sediments sampled at Site (2) are interpreted as characteristic of outer platform-upper slope. Outcrops are dominated by brecciated beds interlayered with stratiform limestone. Breccias beds can be either clast-supported or matrix supported and their thickness can range from a few centimeters to ≈5m (Fig.4). All the breccias are classified using the nomenclature of Woodstock *et al* (2006).

In clast-supported breccias, the

Figure 3.Intrusion of mud and blocky calcite via fractures,remains of gastropod fossil are seen in the upper right side of image(1). Cavity filling mudstone within grainstone(2). Accumulation of brachiopods, shell fragments and bryozoans(3). Large fragment of a crinoid stem(4).

Figure 4. Range of breccia styles, Crackle(1), Mosaic(2) & Chaotic (3) Breccia.

matrix can be either a mudstone or a wackestone, with pack/grainstone clasts. In mud-supported breccias, the mudstone matrix can also be pure mudstone and mudstone containing mudstone microclasts. The heterogeneously-cemented carbonate grains and clasts at site 2 were perhaps par-

tially liquefied or fluidized due to overburden stress and injection of pore water. Although pressurized, the injection was likely triggered by external forces especially seismic events. As a result, well cemented and non-liquefied aggregates of carbonate grain aggregates were transformed into clasts, whereas the liquefied material became trapped as matrix. As well as downslope gravity sliding, periodic faulting and slumping likely played a role in controlling the location of the slope edge and probably in triggering the upslope collapses that initiated debris flows. Bedding strikes 218° and dips 57°.

Joints are the dominant structural components in this area. Two major trends in the mapped fractures are N - S and E - W, with both open and filled fractures. Proximity to abundant breccias, and traces of faulting are indicated by an increase in the density of joint spacing

Site 3/Deep water basin:

The mixed siliciclastic/carbonate rocks of this section mostly comprise limestone blocks embedded in shale, which are interpreted mostly as toe of slope and deepwater environment, embedded in shale in a submarine basin facies, with emplacement of coarser carbonate units more likely during tectonic pulses. Vertically and laterally, the grain-size and proportion of platform derived material decreases across gradational contacts as facies change from slope to deep water pelagic carbonate/siliciclasticassociations. At the toe of the slope a large amount of lithoclasts of varied origins were deposited (Fig.5).Fine-grained pack/wackestones are dominated by fine grained sponge and crinoid fragments. The relative structures produced by different deformation mechanisms.

Probable secondary compressional thrust faults, show slickensides

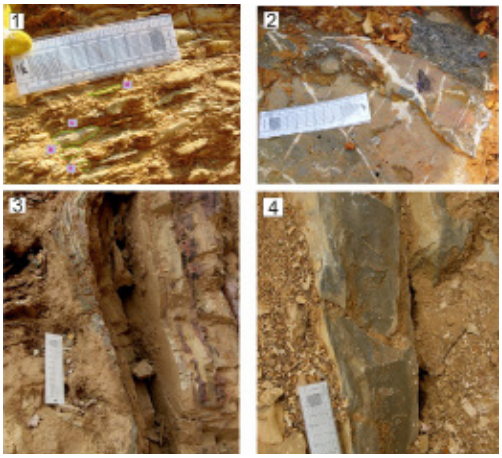

Figure 5. (1)Imbrication of clast and crinoid debris within chaotic slump block shows clast debris (a,b), different proportions of crinoid fragments(c) and bivalve shell(d). (2) different sets of calcite vein. (3) Deformation of shale and interbedded siliciclastic rocks.(4) deep water wacke/mudstone.

on fault planes, calcite occulusion of pores, mineral stepping, and calcite veins preferential along faultplanes parallel to bedding. Siliciclastic bed calcite veins show different variable sets of orientations, the most dominants are 220° to 240°and 110° to 130°. The relative structures produced by different deformation mechanisms. Siliciclastic beds beds with calcite veins show different variable sets of orientations, the most prevalent are 220° to 240°and 110° to 130°.

5. Cement types and diagenetic history

Cement types can be diagnostic of particular diagenetic environments, but caution is required, because identical cement types may be formed in different diagenetic environments(Flugel, 2010). The main types of calcite cement across the three study sites are; bladed, sparry calcite mosasic, fibrous, syntaxial overgrowth and blocky (some with a ferroan-calcite component).

Site 1 textures are mostly highly packed cementstones, microbial boundstones and bioclast grainstones. Peripheral microbial crusts cover parts of the reef/mound fabric. Sometimes these bacterial micrite rinds are reworked into intraclasts, showing the very early nature of this texture. Later diagenetic blocky calcite (including ferroan calcite) consists of medium to coarse grained spar-crystal cement. It filled remaining pore space and likely replaced some earlier cements as petrography shows some blocky spar textures clearly originate via recrystallization of pre-existing cements (Fig.6). Matrix and infilling sediments contain micrite to microspar cement; these micron-sized curved rhombic crystals form rims or thin coatings around grains, can line intraskeletal pores, can fills pores completely or construct bridges between grains.

Marine cements at site 2 show a variety of morphologies, ranging from acicular, columnar to equant crystals. Compared with site 1 there is no evidence of thick early crust of aligned radiaxial calcite cement. Isopachous, bladed calcite cements lining the primary pore space, Matrix is a residue product of pressure solution also shows local micritic cements. Some sparry calcite-filled microfractures are limited to the clasts indicating fracturing prior to brecciation and while others occurred later than brecciation, implying multiple stages of brecciation ranging form early to late. Microbial lime mudstone, crosscut by calcite veins associated with stylolite seams. Non-ferroan calcite is cross-cut by veinlets of blue-stain tinged late stage ferroan calcite.

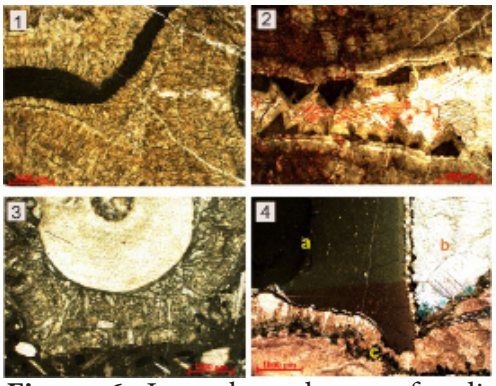

Figure 6. Isopachous layers of radiaxial fibrous cement. Chevron crusts, characterized by V and inverted V-shape patterns (1). Neptunian dyke filling, with sparry layers alternating with micrite layers, Laminated microbial encrusters define the inner boundary of the fissures and the cracks then filled with burial calcite cement. Before then, the fissure edge was cemented by submarine fibrous and radiaxial calcite cements(2). Crinoid fragments show a characteristic cleavage structure. Crinoid fragment is coated by encrusting colonies and bryozoans(3). Skeletal cavity filled with geopetal sediments(a) and late diagenetic blocky calcite (b) that followed biogenic overgrowth and microbial encrustation(c) on skeletal grains.

Isopach fibrous cements on the rim of fractures indicate earlier diagenesis in a marine phreatic environment, which was filled by clear granular and blocky cements that underwent crystal coarsening and recrystallization during burial.

At site 3, deformed clasts show densely packed fabrics that are bound by irregular, anastomosing microstylolitesv(Fig.7). Early cementation of \ the cavities was dominated by blocky

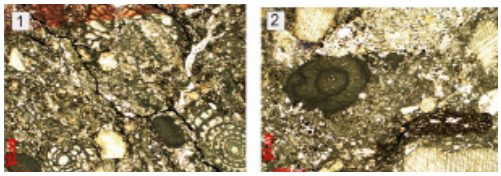

Figure 7. Accumulation of deformed fusulinid & crinoid fragment and clast debris in packstone shows stylolite structure filled by dissolution materials. Grains are densely packed and bound by irregular, anastomosing microstylolites(1). Microboring developed on bivalve shell & degraded algal fragment and former bioclast, some syntaxial crinoids and decomposed bioclast also visible(2).

coarse calcite cements, while in some clasts radiaxial and bladed isopachous cement textures dominate. It seems that blocky cements developed preferentially in open pore spaces. Blocky ferroan calcite and syntaxial overgrowth crinoid fragments are somewhat later stage cements. Etched margins of some calcite cement would suggest, in addition to physical erosion at the edges during crystal silt formation,the calcite spar also underwent some chemical hydrothermal alteration. There is pervasive evidence of partial recrystallization of many of the early cements at site 3. Wackestone and deformed pack/grainstone shows evidence of hydrothermal overprint and quartz vein intrusion. Bioclast wacke/packstone is interbedded with argillaceous laminatedthinly bedded limestone.

6. Isotopic results:

$\delta^{18}O/^{16}O$ versus $\delta^{13}C/^{12}C$ plots from the 3 sites reveal temperature-carbon source relationships that , when related to the sampled textures, become very useful as a tool for interpreting the diagenetic evolution of the region. Precipitation and deposition begin in marine waters (Wang et al. 1996; Saltzman et al. 1998; Kump et al. 1999), passed into the eogenetic, and then into the mesogenetic realms. Rock-fluid equilibration of the isotope signature in the various forms of calcite continues in the burial realm until the rock loses all effective permeability. Hence later burial spars show depleted $\delta^{18}O$ contents.

Site 1 samples show a range of carbon isotopic values (from +4.9 to -3.7 ‰ PDB), whereas the oxygen data range (from -6.1 to -15.8 ‰ PDB). The increasing negative oxygen values indicate a heating trend(Fig.8). This is clearly the result of burial. Likewise most of the matrix cements are related

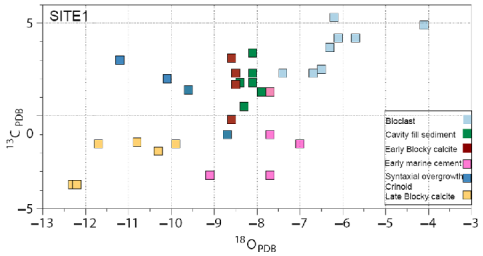

Figure 8.Cross-plot of all carbon and oxygen isotope values at site 1

to cooler (less negative oxygen) portions of the burial indicating and earlier mesogenetic signature. Medial to later burial diagenesis is recorded by the calcite veins in fractures and when vein samples are broken out into earlier versus later they occupy the appropriate positions on the burial curve. Some of the later veins and the late stage calcite spar, with more negative oxygen values also contain ferroan calcite based on stained thin section observation.

Significant depletion in $\delta^{13}C$ associated with these late stage textures (with more negative oxygen) suggests that recrystallization occurred in an open system under the influence of fluids with lighter $\delta^{13}C$ composition. Water supplying cements with lighter $\delta^{13}C$ compositions could have resulted from either organically-charged microbially effected waters or from organic maturation in the burial realm. Microbial activity in the eogenetic to early mesogenetic realms.

At site 2, the isotopic compositions of the rock matrix here too corresponds to a burial history trend (Fig. 9). Once again, crinoid debris has least negative $\delta^{18}O$ values, while some fracture filling and late stage ferroan calcites show most negative (warmer) δ18O values. In the early stage of the burial trend, most of the matrix cement is perhaps related to early marine cementation, whereas void infill sediments show more negative $\delta^{18}O$ values. These infill sediments can contain significant levels of syntaxial overgrowth calcite. The decrease in $\delta^{18}O$ once again indicates increasing temperatures of calcite precipitation with decreasing $\delta^{13}C$ probably indicates increased supply of bicarbonate from decarboxylation reactions at depth. Also the carbon volume within carbonate systems is so large that, unless recharge occurs, the original ^{13}C signature of fluid that enters the burial realm tends to become overprinted by carbon derived from interaction with the host rock, usually with average marine values (Veizer et al,1999., Magaritz and Schulze,1980.,Garrels and Perry, 1974., Schidlowski et al, 1975.,Veizer et al, 1980.,Clark 1980).

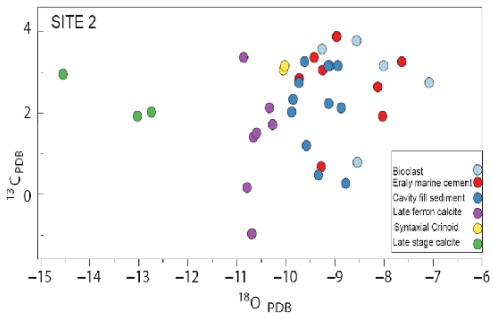

Figure 9. Plot of Carbon Isotope versus Oxygen Isotope for site 2

Oxygen isotope values through the site 3 section fluctuate between −15.7 to −4.3 ‰ PDB and carbon isotope is variable between -7 to 4.8 ‰ PDB (Fig.10). A sample from a calcareous cement volcanic argillaceous interval shows the highest $\delta^{18}O$ PDB value, of -24.7 ‰, due to the high hydrothermal temperature associated with igneous emplacement. Once again calcite with more O-depleted values are most likely the result of continued precipitation at higher temperatures associated with greater burial depths.

7. Discussion:

1. Depositional setting

Field investigation, thin section study, orientation of structures, isotopic and XRD analysis provide a comprehensive set of data for that can be integrated to better understand the contrasting depositional and diagenetic complexity in the deep through shallow water successions in the Permian carbonates, which were the focus of this study. Deposition at Site 1 (Temple) constructed a massive limestone with abundant muddy boundstone textures, it is the result of a combination of waves and currents interacting with its shallow reef building community and associated microbial encrusters and cementers. This biota, along with the highly CaCO3 saturated tropical waters that typified Permian oceans, combined to construct cementstones, microbial boundstones and bioclast grainstones, along with some early eogenetic cement-lined fractures or neptunian dykes.

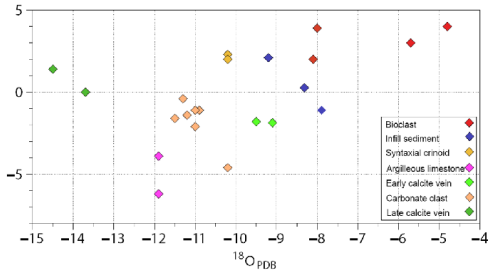

Figure 10. Carbon and oxygen isotopic composition of site 3

Site 2 (farm) is interpreted as a outer platform/ upper shelf succession, composed of bioclast pack/grainstone, microbial grain/packstone, along some skeletal and boundstone debris derived from the nearby shallower platform. The succession is extensively brecciated, often is association with injectite breccia textures cutting across relatively undisturbed beds. Brecciation could be due to the clastic loading and clastic soft sediment injection,or perhaps more probably a response to seismically induced faulting and associated slumping and collapse of pressurized outer platform upper slope sediments.

Site 3 (quarry) Limestone, with its dominantly hydrothermal affected wackestone, mudstone and altered packstone texture abundant in crinoid fragment interpreted to represent a deeperwater facies which was deposited under toe of slope and deeper basinal setting.

2. Diagenetic history:

The diagenetic features of the site 1 and 2 with their suggest that the sediments across platform to deeper basin setting have undergone a broadly similar pattern of syn- and post-depo-

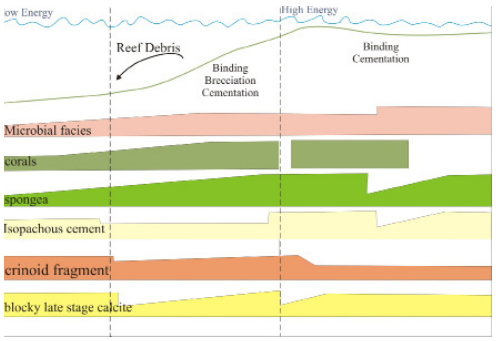

Figure 11. Idealized transect of the three outcrops showing the trends in microfacies composition and diagenetic evolution of the different carbonate facies

sitional events. In approximate order of occurrence, these events are: 1) Micritization and early marine cementation with intense microbial activity, 2) Replacement of some algae, coral, sponge and crinoid fragment, particularly at their edges during the precipitation of cements 3) Development of fractures, stylolites and spar calcite 4) replacement of original metastable carbonate with radiaxial and fiber calcite spar and loss of most remaining primary pore-space during shallow burial; and 5) Formation of later stage calcite, overgrowth texture and the passage of burial fluids through remaining conduits. Site 3 (quarry) limestone, with its dominantly hydrothermal overprinted wackestone, mudstone and altered packstone texture abundant in crinoid fragment interpreted to represent a deeperwater facies which was deposited under toe of slope and deeper basinal setting.

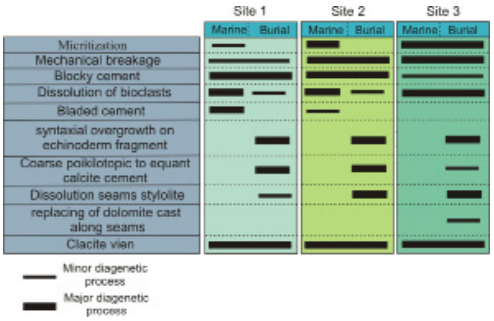

Figure 12. Sequence of diagenetic events affecting the shallow water platform to deep water basin successions.

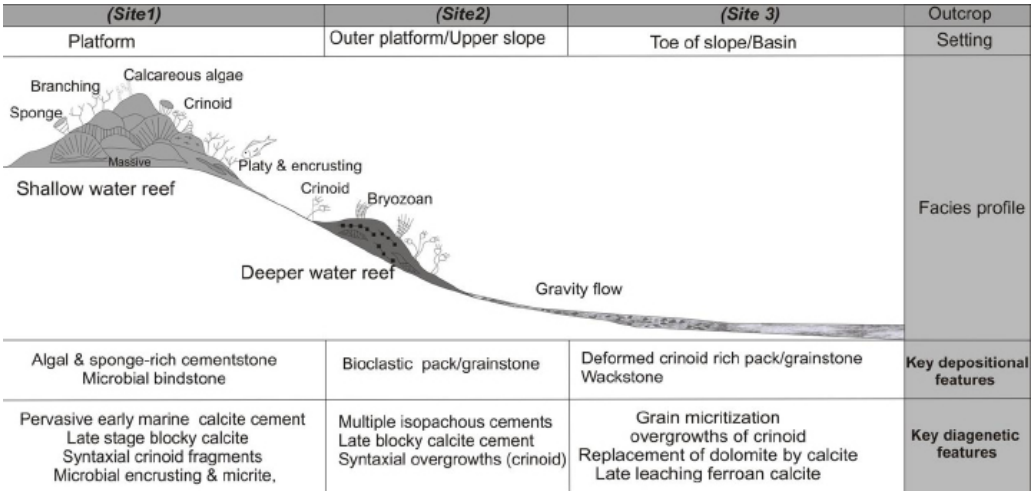

Figure 13.Depositional features, diagenesis and hydrothermal infl uence of carbonate system from shallow to deep water setting

Results of the diagenetic analysis shows that some crinoid and sponge fragments, inner cements in Neptunian dykes and some fractures, are marine in origin, and formed at lower burial temperatures. Cavities and fissures were cemented prior to cementation of at least parts of the fine-grained matrix itself, which was later cemented by $CaCO_3$ derived from wamer hydrothermal or later burial fluids with more negative oxygen values. The carbonate host seen in many breccia, although plastic, was cohesive enough to be fractured before matrix cementation. There also remains some equilibration phases of earlier

calcite vein and spar cements within the infi llment sediments. Depletion in δ13C in some parts can be explained by higher temperature hydrothermal fluids during precipitation, or the mor enegative carbon could come from secondary enrichment via volatile mobilisation from organic matter at catagenic temperatures and/or from earlier high levels ofthe marine microbial productivity along encrusting layers and grain rinds.

Acknowledgments

Sincere thanks goes to Chulalongkorn University; Chevron-PTTEP International Master Program in Petroleum Geosciences, Department of Geology and Faculty of Science Chulalongkorn; and to my supervisor Prof. Dr. John Keith Warren for all of his patience and supervision, and to the program director Dr. Joseph Lambiase; also thanks to Dr. Thasinee Charoentitirat and Prof. Dr. Philip Rowell for all their valuable guidance.

References

Ahr, W. M., 2008, Geology Of Carbonate Reservoir. The Identifi cation, Description, and Characterization of Hydrocarbon Reservoirs in Carbonate Rocks: Hoboken, New Jersey, John Willey and Sons, 277 p.

Callot, P., F. Odonne, and T. Sempere, 2008, Liquifi cation and soft-sediment deformation in a limestone megabreccia: The Ayabacas giant collapse, Cretaceous, southern Peru: Sedimentary 41,Geology, v. 212, p. 49-69.

Dunham, R. J., 1962, Classifi cation of carbonate rocks according to depositional texture,Classification of Carbonate Rocks, Memoir of American Association of Petroleum Geologists,v.1, p. 108-121.

Flugel, E., 2010, Microfacies of Carbonate Rocks,Analysis, Interpretation and Application,Springer-Verlag Berlin Heidelberg, 984 p.

Hoefs, J., 2009, Stable Isotope Geochemistry (6th Edition), Springer, Berlin, 285 p.

Hunt, D. W., W. M. Fitchen, and E. Kosa, 2003, Syndepositional deformation of the Permian Capitan reef carbonate platform, Guadalupe Mountains, New Mexico, USA: Sedimentary Geology, v. 154, p. 89-126.

L. F. Montaggioni, and C. J. R. Braithwaite, eds, 2009, Quaternary Coral Reef Systems: History,Development Processes and Controlling Factors: Developments in Marine Geology, v.Volume 5, Elsevier, p. iii.

Liao, W., Y. Wang, S. Kershaw, Z. Weng, and H. Yang, 2010, Shallow-marine dysoxia across the Permian–Triassic boundary: Evidence from pyrite framboids in the microbialite in South China: Sedimentary Geology, v. 232, p. 77-83.

Morley, C. K., P. Ampaiwan, S. Thanudamrong, N. Kuenphan, and J. Warren, 2013, Development of the Khao Khwang Fold and Thrust Belt: Implications for the geodynamic setting of Thailand and Cambodia during the Indosinian Orogeny: Journal of Asian Earth Sciences, v. 62,p. 705-719.

Mort, K., and N. H. Woodcock, 2008, Quantifying fault breccia geometry:

Dent Fault, NW England: Journal of Structural Geology, v. 30, p. 701-709.

Shen, J.-W., G. E. Webb, and J. S. Jell, 2008, Platform margins, reef facies, and microbial carbonates;a comparison of Devonian reef complexes in the Canning Basin, Western Australia,and the Guilin region, South China: Earth-Science Reviews, v. 88, p. 33-59.

Tucker, M. E., and P. Wright, 1990, Carbonate sedimentology: Oxford, Blackwell Science, 482p.

Ueno, K., A. Miyahigashi, Y. Kamata, M. Kato, T. Charoentitirat, and S. Limruk, 2012, Geo47 tectonic implications of Permian and Triassic carbonate successions in the Central Plain of Thailand: Journal of Asian Earth Sciences, v. 61, p. 33-50.

Wilson, M. E. J., 2002, Cenozoic carbonates in Southeast Asia: implications for equatorial carbonate development: Sedimentary Geology, v. 147, p. 295-428.

Yılmaz, C., 2006, Platform–slope transition during rifting: The mid-Cretaceous succession of the Amasya Region (Northern Anatolia), Turkey: Journal of Asian Earth Sciences, v. 27, p.194-206.

Zampetti, V., W. Schlager, J.-H. van Konijnenburg, and A.-J. Everts, 2004, Architecture and growth history of a Miocene carbonate platform from 3D seismic refl ection data; Luconia province,offshore Sarawak, Malaysia: Marine and Petroleum Geology, v. 21, p. 517-534.